U.S. Fish and Wildlife Service Final Report: Bald Eagle Population Size: 2020 Update

U.S. Fish and Wildlife Service Final Report: Bald Eagle Population Size: 2020 Update

December 2020

Collaborators (Alphabetical Order):

Cornell University Laboratory of Ornithology: Orin Robinson, Viviana Ruiz-Gutierrez, Erica Stuber

New Mexico State University Department of Fish, Wildlife, and Conservation Ecology: Fitsum Abadi, Jay Gedir

U.S. Geological Survey: William Kendall, Colorado Cooperative Wildlife Research Unit; John Sauer, Patuxent Wildlife Research Center

U.S. Fish and Wildlife Service Division of Migratory Bird Management: Emily Bjerre, Brian Millsap, Mark Otto, Joel Pagel, Guthrie Zimmerman

Cover Photo: Banded adult bald eagle (*Haliaeetus leucophalus*) by Barbara Pierzakowski, Audubon Center for Birds of Prey EagleWatch Program.

EXECUTIVE SUMMARY

This report is a technical update of the scientific information for bald eagles published in the U.S. Fish and Wildlife Service's (Service) Programmatic Environmental Impact Statement for the Eagle Rule Revision (PEIS), which was finalized in December 2016. In the PEIS, the Service committed to updating population size estimates for both bald and golden eagles no less than once every six years. This report fulfills that commitment for bald eagles in the coterminous United States for four of six eagle management units (EMU) – the Atlantic Flyway, Mississippi Flyway, Central Flyway, and Pacific Flyway North EMUs.

There were three major components to this technical update: (1) aerial surveys in 2018 and 2019 of 364 plots (10 by 10 km^2) to estimate the number of occupied bald eagle nesting territories in 16 high-density breeding survey strata; (2) developing a model to relate eBird bald eagle relative abundance estimates to the survey-based occupied nesting territory estimates at the plot level, and then using the eBird model and eBird data to estimate the number of occupied bald eagle nesting territories for four of the six EMUs; and (3) using an integrated population model (IPM) to obtain updated estimates of bald eagle vital rates, and then using these estimates to expand the estimates of numbers of occupied bald eagle nesting territories to estimates of total population size. This report is divided into three parts: Part 1 provides details on the aerial survey and plot-based estimates; Part 2 describes how we developed the model to use eBird relative abundance data to estimate occupied bald eagle nest density; and Part 3 describes the IPM and results.

We estimated 316,700 bald eagles were present in the four EMUs in the 2019 breeding season, 4.4 times more eagles than in 2009. This indicates the bald eagle population has continued to increase rapidly since our previous survey. Our IPM also allowed us to better incorporate floaters, juveniles, and subadults into estimates of overall population size, which we could not do effectively with the previous efforts, and this also contributed to the increase. Consistent with our commitment in the 2016 PEIS, we recommend continued monitoring with a frequency of no less than one update every six years.

PART 1

DUAL-FRAME BALD EAGLE OCCUPIED NEST SURVEY RESULTS: 2018-2019

Contributors: Mark Otto, John Sauer, Emily Bjerre, Guthrie Zimmerman, Joel Pagel, and Brian Millsap

In 2018–2019, the Service conducted the second national survey to estimate the total number of occupied bald eagle nesting territories in the coterminous U.S. The survey replicated the 2009 national bald eagle nesting survey, following the same dual-frame sampling design modified to account for detectability of nest structures. The dual-frame survey divided the coterminous U.S. into strata based on the abundance of nest structures and sampled high abundance areas for the number of occupied nests. We collaborated with the Cornell Lab of Ornithology to relate plot-level estimates of occupied nesting territories from the survey with eBird relative abundance estimates and then predict the total mean number of nesting territories accounting for model estimation uncertainty for each Service bald eagle management unit (see Part 2). The dual-frame survey estimated 31,304 (SE 2,511) occupied nesting territories for all surveyed areas (i.e. areas with the highest abundances of known nesting territories. The substantial increase in the number of occupied nesting territories in surveyed strata from 2009 estimates reflects these improvements in estimation methods in addition to increases in the number of breeding pairs of bald eagles.

SURVEY OVERVIEW

U.S. Fish and Wildlife Service (2009 and 2016) developed a plot-based national-scale aerial survey to monitor the status of the bald eagle by collecting occupancy data on nest structures (nests). Occupied nests are equivalent to occupied nesting territories since there is only one occupied nest structure per nesting territory (see Steenhof and Newton 2007). The 2009 baseline survey provided the first unbiased national estimate of the number of occupied bald eagle nests and a baseline for detecting population change with future surveys. The 2018–2019 survey was a repeat of the 2009 survey, with some changes to improve survey efficiency. The dual-frame survey design takes advantage of the efficiency of surveying known nest locations and uses randomly selected area plot searches to account for nests not included on the lists. The survey also accounts for detectability of nests using an independent double-observer protocol and correcting for detection probability.

Previously, estimates of bald eagle population size combined the dual-frame estimates for the surveyed areas of highest known bald eagle nest densities (i.e. the survey strata) with minimum known counts from local monitoring efforts to estimate total management unit occupied nesting territories (U.S. Fish and Wildlife Service 2016). For this analysis, we were able to improve estimates by working with Cornell Lab of Ornithology to relate our plot-based survey estimates with eBird relative abundance estimates and use that model to predict the number of occupied nesting territories for each bald eagle management unit in the coterminous U.S. (see Part 2). These estimates should better represent the number of occupied nesting

territories, in particular for areas with low-densities of known nest structures that were not feasible to sample with the aerial survey.

Survey design

The dual-frame survey design provides a means of using the existing data on the number of occupied nests available from state lists (the 'list frame') and estimating the number of additional occupied nests not accounted for by the lists. This requires sampling survey plots (the 'area frame') for occupied nests, removing known nests (those on the lists) from the samples, and estimating the number of occupied nests that are not on the lists. The number of new, occupied nests are then added to the occupied nests from the lists to get the total number of occupied nests. Since not all nests are seen during sampling, we account for detection probability of nests during the area sampling using a multiple-observer procedure. Bald eagle abundance also varies greatly within the coterminous U.S. and plot surveys could only be implemented in areas where bald eagle nesting populations were large enough that they could be surveyed with reasonable effort.

The 2009 survey was designed to give an 80% chance of detecting a 25% change between surveys at a 10% significance level over the whole survey area, requiring an 8.3% coefficient of variation (CV) of the dual-frame estimate of total occupied nesting territories. We allocated the frame and stratum sample sizes to minimize overall cost with an upper limit on the overall CV.

Stratification and sampling effort

We repeated the area stratification from the 2009 survey, which was based on a cluster analysis of bald eagle nest densities (Figure A3-1, U.S. Fish and Wildlife Service 2009). We selected area-frame sample plots for the survey using the Generalized Random Tessellation Stratification (GRTS) methodology (Kincaid and Olsen 2013). We used the list-frame compiled for the 2009 survey since many states had discontinued formal efforts to regularly check nests or formally update state nest lists. The strata list-frame estimates are combined with the area-frame survey estimate (corrected for detectability of nests based on multiple observer procedures) to compute the dual-frame estimates. Therefore, we anticipated use of the older list nest would result in the list frame contributing less to the dual-frame estimate and reduced benefit from using the dual-frame versus area-only estimates. We selected list plots based on the per-plot means and standard deviations of the number of nests per stratum. List sampling included any known nests included in GRTS-selected area sample plots and additional list sample plots.

We used simulations to optimize flight costs within our precision requirements and operational constraints to determine the final sample selection based on data from the 2009 survey effort. Due to anticipated degradation of the list coverage (proportion of total nests represented on the list) over time, all plots selected for the list-frame were also flown as area sample plots. We drew an over-sample for each sampling frame by strata; these were replacements for selected plots that could not be flown for a variety of access, safety, or logistical issues.

Surveys

We conducted survey flights in the early part of the breeding season when the majority of bald eagle breeding pairs are closely tied to nests and detectability should highest (before leaf-out). Survey crews recorded GPS locations and nest status observations following protocols described in the post-delisting monitoring plan (U.S. Fish and Wildlife Service 2009). Post-survey, we used flight tracks and nest information to reconcile nest observations with known nests and determine the sampling frame assignment and status for each nest (see U.S. Fish and Wildlife Service 2016 for additional detail). We flew strata in the Service's Mississippi Flyway management unit in 2019 and all other strata in 2018.

Estimation

To estimate the number of occupied nesting territories in the survey strata, we extended the 2009 dual-frame survey model (U.S. Fish and Wildlife Service 2016) with random effect for strata and random effects for plots with a constant standard error (SE) among all strata. Known nests were removed from the area sample and made part of the list sample prior to data analyses to ensure independence of the two data frames. We used Bayesian estimation with non-informative or diffuse priors to obtain all estimates.

To extrapolate to list nests in the unsampled plots in the strata, we predicted occupied/not occupied proportions with the stratum random effect mean and SE using the beta distribution then predicted the number of occupied nests using a binomial distribution. The same plot proportions were used for unchecked list nests in sample plots. All occupied nests were summed to get the stratum-level list totals. We did not have enough observations to account for imperfect detection in known nests and thought the observation process was too different to assume it was the same as for new nests.

For the area frame, we estimated the per-plot densities of new nests for each plot by stratum. By 'new', we mean new to the list, not necessarily newly constructed (e.g., one could observe a well-established nest that is clearly 'old' but previously unknown, especially in areas not traditionally included in state surveys). New nests found in 2009 were added to the list frame for 2018–2019. We predicted log-normal densities with the stratum random effect mean and SE using the beta distribution then predicted the number of occupied nests using a binomial distribution. We used independent, double-observer counts to account for observer detection (Royle and Dorazio 2008:176). From the record of capture histories, we estimated a mean likelihood with centered platform effect, centered seat effect, and a random observer effect. We used a gamma-normal approximation of a uniform on the logit scale for the observer effect to make a main-effect model for observer detection. The resulting likelihood is a multinomial with the combination of observer in each seat and a log scale plot random effect with constant SE for both the sampled and unsampled plots. Again, the sampled and unsampled plot estimates of occupied nesting territories are summed for the stratum totals.

Area-only estimation

We also generated an estimate of the stratum extrapolation from the area-plot counts only (as though there were no list data) for comparison with the dual-frame estimate. We used all nests observed in the area plots (including list nests) and the observer-detection correction to calculate the totals and standard errors as described above and compared estimates to the list-only and dual-frame estimates. Applying the observer-detection correction to the known list nests may make estimates slightly high since detection rates may be higher than for unknown nests. Similar numbers of sampled area plots relative to the effort put into the list sample are also important in order to make a reasonable comparison between the estimates.

Dual-frame estimation

Since the estimates of occupied, known nests from the list frame and the estimates of occupied, new nests from the area-frame are independent, we sum the totals and their variances to get the dual-frame estimates (U.S. Fish and Wildlife Service 2009, 2016). We added the list-frame and area-frame stratum estimates to get the total following Haines and Pollock (1998). We similarly added the variances to get the variance of the total.

List coverage

The list coverage is the percent of the total estimated nests (irrespective of occupancy status) that were represented in the list frame; it highlights the relative number of nests represented on (or missing from) the list. The number of nests in the list is fixed, but the number of new nests is estimated. We simulated the new nest distribution with a log normal with the log mean of the new nest estimate and its relative variance. The means and standard errors are taken from simulations.

RESULTS

The 2018–2019 survey was designed to replicate the 2009 survey and estimate the total number of occupied nesting territories for bald eagles in the survey strata using a dual-frame approach (unbiased and explicitly accounts for uncertainty). Stratification using known nest densities and physiographic boundaries helped ensure representative, efficient sampling and estimation which are important given the survey goals and highly variable bald eagle abundance within the U.S.

There were 478 occupied list nests out of the total 1,332 list nests sampled. List nest occupancy rates ranged from 29–46% among strata and averaged approximately 35%. Within strata, we extrapolated the list nest occupancy rates and standard errors for the sampled nests to the nests not included in the sample to get the total occupied nests for the list-frame—5,469 (SE 281) occupied nesting territories (Table 2).

There were 720 new, occupied nests recorded by survey crews. Detection rates varied by observer-seat-platform combination with the probability of at least one observer detecting a nest ranging from as low as 71% (SE 3.2%) to as high as 98% (SE 0.5%). Platform had a noticeable impact on detectability, with helicopter crew detection rates of 96% (SE 1.1%) to 98% (SE

0.5%). This was consistent with the general impression of survey crews that searching for nest in helicopters was more accommodating in terms of general maneuverability and visibility in spite the helicopters often being used for plots with habitat that would be considered to have lower detectability (e.g. conifer-dominant tree stands). Accounting for detection, estimates of new, occupied nest ranged from 113 (SE 62.5) in Washington Southern Cascades to 6,787 (SE 1,248) in the Boreal Transition, which is the northern part of the Great Lakes region (Table 2).

Dual-frame estimates represent the total occupied nests for each stratum and ranged from 162 (SE 64) occupied nests in the Washington Southern Cascades to 8,228 (SE 1,257) occupied nests in the Boreal Transition area in the northern portion of the Great Lakes region. In total, for all of the high-density strata combined, we estimated 31,304 occupied nests (SE 2,511).

To evaluate the efficacy of the dual-frame survey and better understand the contribution of each sample frame to the analysis, we also analyzed the area survey plot data as though we only conducted the area plot survey (Table 2). The area-only estimates are generally consistent with the dual-frame estimates but deviate in some strata (generally those strata with a large number of list nests).

ACKNOWLEDGEMENTS

LITERATURE CITED

Gelman, A., J. B. Carlin, H. S. Stern, and D. B. Rubin. 1995. Bayesian Data Analysis, 1st edition. London, Chapman & Hall.

Givens, G. H., and J. A. Hoeting. 2005. Computational Statistics. John Wiley & Sons, Inc.

Haines, D. E., and K. H. Pollock. 1998. Estimating the number of active and successful bald eagle nests: an application of the dual-frame method. Environmental and Ecological Statistics 5:245–256.

Kincaid, T. M., and A. R. Olsen. 2013. spsurvey: spatial survey design and analysis. R package version 2.6.

Link, W. A., and R. J. Barker. 2010. Bayesian Inference with Ecological Applications. Academic Press, London, United Kingdom.

Plummer, M., 2003. JAGS: A program for analysis of Bayesian graphical models using Gibbs sampling. Page 10 in K. Hornik, F. Leisch, and A. Zeileis, editors. Proceedings of the 3rd International Workshop on Distributed Statistical Computing (DSC 2003). Vienna, Austria.

Royle, J. A, and R. M. Dorazio. 2008. Hierarchial Modeling and Inference in Ecology. The Analysis of Data from Populations, Metapopulations and Communities. Academic Press, London, United Kingdom.

Sauer, J. R., J. E. Hines, J. E. Fallon, K. L. Pardieck, D. J. Ziolkowski, and W. A. Link. 2014. The North American breeding bird survey, results and analysis 1966–2012, version 02.19.2014. USGS Patuxent Wildlife Research Center, Laurel, MD. URL http://www.mbr-pwrc.usgs.gov/bbs/bbs.html.

Steenhof, K., and I. Newton. 2007. Assessing raptor reproductive success and productivity. Pages 184–192 in K. L. Bildstein and D. M. Bird, editors. Raptor research and management techniques. Hancock House, Surrey, B.C.

Thompson, S. K. 1992. Sampling. John Wiley & Sons, Inc., Hoboken, New Jersey, USA.

U.S. Fish and Wildlife Service. 2009. Post-delisting monitoring plan for the bald eagle (*Haliaeetus leucocephalus*) in the contiguous 48 states. U.S. Fish and Wildlife Service, Divisions of Endangered Species and Migratory Birds and State Programs, Midwest Regional Office, Twin Cities, Minnesota, USA.

U.S. Fish and Wildlife Service. 2016. Bald and Golden Eagles: Population demographics and estimation of sustainable take in the United States, 2016 update. Division of Migratory Bird Management, Washington D.C., USA.

U.S. North American Bird Conservation Initiative Committee. 2000. North American bird conservation initiative bird conservation regions map. Division of Migratory Bird Management, U.S. Fish and Wildlife Service, Arlington, Virginia, USA. URL http://www.nabci-us.org.
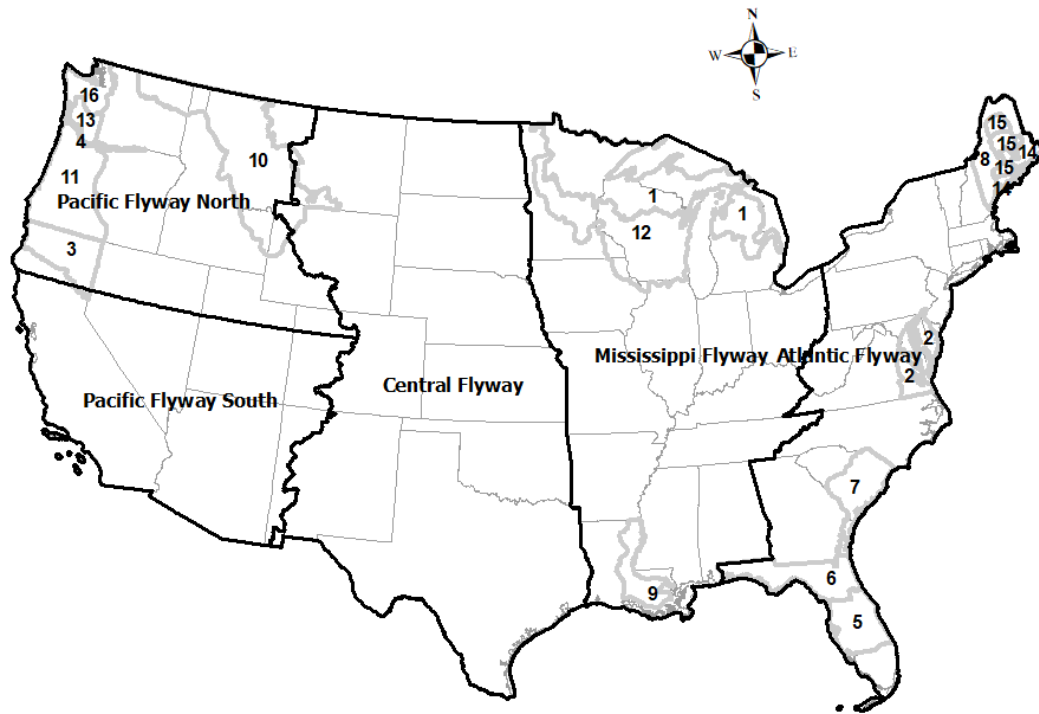
Figure 1. Bald eagle management units and survey strata. Management units are defined by the dark lines, and are labeled on the figure. Survey strata are 1 = Boreal Transition, 2 = Chesapeake Bay, 3 = California Highlands, 4 = Columbia River, 5 = Central Florida, 6 = Northern Florida, 7 = Southeastern Lowlands, 8 = Maine Lowlands, 9 = Mississippi Valley, 10 = Northern Rockies, 11 = Oregon, 12 = Prairie Transition, 13= Southern Cascades, 14 = Upper Atlantic Coast, 15= Maine Highlands, 16 = Western Cascades.

Table 2. Mean (SD) list-only, area-only (new nests), and dual-frame estimates of occupied nesting territories from aerial surveys (2018–2019) by survey strata—the regions of the coterminous U.S. with the highest known densities of nest structures.

Stratum	List-only		Area-only		Dual-Frame	
Washington Southern Cascades	49	(13)	113	(63)	162	(64)
Olympic Puget Sound and NE Cascades	770	(97)	440	(128)	1,209	(162)
Columbia River	140	(32)	115	(56)	255	(64)
Oregon Pacific Rainforest	474	(69)	973	(313)	1,448	(321)
California High Density	47	(11)	866	(415)	914	(415)
Northern Rockies	214	(39)	3,284	(1013)	3,498	(1,013)
Boreal Hardwood Transition	1,441	(144)	6,787	(1248)	8,228	(1,257)
Prairie Hardwood Transition	272	(44)	4,733	(1053)	5,005	(1,054)
Mississippi Alluvial Valley in Louisiana	217	(20)	2,760	(631)	2,978	(631)
Maine Upper Middle Coast and Highlands	60	(13)	239	(114)	298	(115)
Maine Low	76	(16)	493	(271)	568	(272)
Maine Down-East	426	(87)	335	(174)	761	(195)
Chesapeake Bay	428	(41)	2,046	(414)	2,474	(416)
South Carolina-Georgia Lowlands	136	(16)	801	(220)	937	(221)
Central Florida	445	(58)	840	(220)	1,284	(227)
North Florida	276	(29)	1,009	(282)	1,285	(284)
Total	5,469	(281)	25,835	(2,495)	31,304	(2,511)

11

PART 2

METHODS FOR INTEGRATING EBIRD RELATIVE ABUNDANCE DATA WITH

POPULATION SIZE DATA TO PRODUCE SPATIALLY EXPLICIT ESTIMATES OF

EAGLE DENSITY

Contributors: Erica Stuber, Emily Bjerre, Brian Millsap, Mark Otto, Orin Robinson, Viviana Ruiz-Gutierrez, Guthrie Zimmerman

The goal of this collaboration between the Service and Cornell Lab of Ornithology was to determine whether scientific products predicting bald eagle relative abundance developed by the Cornell Lab of Ornithology can be used to predict the number of occupied bald eagle nesting territories across the U.S. While the Service has developed a study design for collecting data regarding bald eagle nest density across the coterminous U.S. and analytical techniques to extrapolate estimates to unsurveyed locations, the higher spatial and temporal resolution of eBird abundance products could be beneficial to the Service's internal management decision-making. However, as eBird predicts the mean relative abundance of total bald eagles (i.e., including juveniles, and adults), and the Service estimates the mean number of nests, the units of each dataset are not directly equivalent, and a statistical relationship must be quantified. To quantify the relationship (if any) between the two quantities, we followed the following steps: (1) formulate a model that related eBird relative abundance to FWS-based estimates of mean number of nests which may vary geographically, and that can predict at arbitrary spatial scale; (2) perform variable selection on a subset of possible eBird relative abundance covariates; (3) confirm the predictive performance of the model based on spatially stratified holdout data; (4) estimate the relationship between eBird mean predicted relative abundance and the Service's estimated mean nest density; and (5) project estimated model across the coterminous U.S. to predict total mean number of nesting territories accounting for model estimation uncertainty.

METHODS

Formulating the model

Because the Service was interested in predicting the mean number of occupied nesting territories potentially at multiple spatial scales depending on specific management objectives (e.g., within the coterminous U.S., flyway scale, or Bird Conservation Region scale), we designed a statistical model that would be valid when projected across arbitrary spatial scales (i.e., the sum of the predicted mean number of nests at two neighboring 10×10 km^2 sites would be the same as the mean number of nests predicted from a single 20×10 km^2 site):

$$N_i \sim \text{Poisson}(\beta_1 \, eBird_i * \exp(\gamma Stratum\_i)).$$

Here, we fit an identity-link Poisson regression model without an intercept, and including the random effect of geographic region of the survey (i.e., Stratum). Suppressing the intercept ensures that when eBird predicted mean relative abundance is zero, the model does not predict

that there are any nests. The Poisson distribution with identity link ensures that predictions can be made at arbitrary spatial scales as both the Poisson mean and variance can be summed. Including the random effect as a multiplicative term guarantees that within each stratum, the intercept goes through the origin, and therefore acts as a random slope by region. N_i represents the estimated mean number of occupied nesting territories in the ith 10×10 km^2 survey plot rounded to the nearest integer to fit the Poisson distribution; these values were obtained from the analyzed aerial survey data as described in Part 1. β_1 represents the coefficient estimate of the eBird-based estimated mean relative abundance predictor (eBird$_i$). eBird$_i$ represents the predicted mean relative abundance of bald eagles at the 10 km^2 scale for plot i. As eBird-based relative abundance products are originally generated at a 2.7 km^2 scale, to match the size of Service aerial survey sites we aggregated the original eBird predicted mean relative abundance to 10 km^2 resolution by taking the sum (R package: raster, function: extract). Because the rate parameter of the Poisson distribution must be strictly positive, we add 0.001 to the eBird covariate to ensure strict positivity under the Poisson distribution with no intercept and only a single fixed covariate (e.g., if any entry of eBird$_i$ = 0, the rate parameter would also be 0, which is not allowable). γStratum_i represents the coefficient for a plots' stratum grouping variable.

Variable selection

We performed a cross-validation procedure in a variable-selection framework to determine which week of predicted eBird mean relative abundance was the best single predictor of occupied nesting territories (see below for cross-validation description). Although eBird relative abundance products contain weekly estimates (i.e., 52 potential predictor variables), we only considered weeks 19-25 as potential predictors in our model as these include the average expected breeding season dates, and are few enough to worry little about multiple testing. Within the cross-validation we only allowed a single predictor to be included at one time (e.g., we did not consider both weeks 19 and 20 simultaneously within our model). We selected the single predictor with the best holdout predictive performance which we then used to estimate the final model using the full data set.

Confirm predictive performance

Because we were interested in using this model to predict the expected mean number of occupied bald eagle nesting territories in both surveyed and unsurveyed regions, we quantified the predictive performance of our model using spatial holdout data in x-fold cross-validation. Each fold of the cross-validation procedure was comprised of all survey sites from within a single stratum (i.e., spatially clustered data). For each fold of cross-validation, we predicted the mean number of nests within holdout sites from a single stratum using the fitted model. After all strata were used as holdout samples we quantified predictive performance as the difference between predicted and observed during holdout, and selected the single model with the greatest predictive performance.

Estimate relationship

Using the model with the highest predictive performance, we estimated the model using the full dataset via posterior simulation with JAGS (Plummer 2013). We used relatively vague priors, and 50,000 iterations, after 25,000 iterations of burn-in, and visually inspected trace-plots to confirm convergence.

Project estimated model across the coterminous U.S.

Once the model was estimated, we projected the estimated model across the coterminous U.S. to determine the total expected mean number of nests in the U.S. and in each major flyway based on the eBird 2018 status and trend product which has continuous spatial coverage for the U.S. To quantify point estimates and uncertainty around the predicted total mean number of nests we generated predictions based on each iteration of the MCMC chain (i.e., for each MCMC iteration we have a separate coefficient estimate; instead of predicting based on the posterior median only, we account for coefficient uncertainty by summarizing over all possible coefficient estimates). Because we were interested in the median and 20th quantile estimates of total mean number of nests, and because we can only extract uncertainty around the median point estimate from the MCMC sampling procedure (i.e., the credible interval from a MCMC chain is only guaranteed to be around the median), we use bootstrapping to generate uncertainty estimates also for the 20th quantile. Based on 50,000 predictions of total mean number of nests we draw 1,000 samples of 1,000 size each, which we summarize for the median and 20th quantiles, as well as their standard deviation. The estimated number of occupied bald eagle nesting territories from our eBird model are presented in Part 2 Results, Table 1.

RESULTS

Our model that integrated eBird relative abundance estimates with bald eagle occupied nesting territory estimates for the surveyed strata produced an estimate of 73,499 occupied nesting territories in the four EMUs in 2018-2019 (Table 1).

Table 1. Estimates of occupied nests from integrated aerial survey and eBird relative abundance data by bald eagle management unit, 2018 – 2019.

Region	Occupied Nesting Territories		
	Mean	SD	Median (20th Quantile)
Atlantic Flyway	19,685	142	19,074 (15,691)
Central Flyway	7,167	71	6,867 (5,197)
Mississippi Flyway	36,973	219	36,038 (30,967)
Pacific Flyway North	9,674	52	9,488 (8,239)
Total	73,499	275	71,467 (60,094)

PART 3

AN INTEGRATED POPULATION MODEL TO INFORM ALLOWABLE TAKE of BALD

EAGLES

Contributors: Guthrie Zimmerman, Fitsum Abadi, Jay Gedir, William Kendall, and Brian Millsap

The Service agreed to use the most current demographic and population data to update estimates of allowable take for bald eagles from the 2016 assessment (U.S. Fish and Wildlife Service 2016a). Based on the biology of eagles and management structure of the Service, the Service manages eagle populations based on eagle management units (EMUs) that mostly follow the administrative flyways in the conterminous U.S., with the exception of the Pacific Flyway (PF), which is divided into northern and southern sections at 40° N latitude (Figure 1; there is also an Alaskan management unit that is not considered here). The subpopulation of bald eagles in the southern PF largely occupy the Sonoran and Mojave Deserts, Sierra Madre Occidental, and southern portion of the Southern Rockies Colorado Plateau Bird Conservation Regions (BCRs; U.S. Fish and Wildlife Service 1998) of Arizona. This southern PF population is managed separately from the rest of the U.S., so we excluded those birds from this assessment (U.S. Fish and Wildlife Service 2007). The Service implemented a nest occupancy survey for bald eagles in 2009 following removal from the list of Threatened and Endangered species (U.S. Fish and Wildlife Service 2009). For the purposes of surveying nesting territories, the remainder of the conterminous U.S. was divided into low- and high-density areas based on available data on nesting density from 2009 (U.S. Fish and Wildlife Service 2016a). The high-density bald eagle areas were further divided into 16 strata based on the intersection of BCRs and states (U.S. Fish and Wildlife Service 2009; Figure 1). We used data from these regions to update estimates of demographic data for bald eagles in these EMUs.

DATA AND MODEL

Bald eagles are banded throughout the U.S. as part of operational monitoring, or specific studies. Bald eagles are captured and banded with uniquely numbered aluminum leg bands, and often with additional markers (e.g., colored leg bands, satellite transmitters). Occasionally, dead eagles that are banded with only aluminum leg bands and no other markers are located and the band numbers are reported to the Bird Banding Laboratory (U.S. Geological Survey Bird Banding Laboratory 2019). These banding and recovery data (i.e., band recovery data) provide information on survival rates. We attempted to use live resightings of color bands to increase precision because bald eagle band recoveries are sparse, but our initial assessment of the live-resight data indicated large heterogeneity in resighting efforts that could have induced an unknown bias into estimates. Therefore, we excluded live-resight information until we could conduct a more detailed assessment about using these data appropriately. We also excluded birds tagged or marked with transmitters, wing, tail, or other markers that might influence survival or bias reporting probabilities.

We define recruitment as the number of female juveniles fledged per adult female, and estimate recruitment as the product of the probability of after third year (AY3) birds breeding

(*p.br*) and fecundity (female young fledged per breeding female; *F*; Steenhof and Newton 2007). Bald eagle recruitment is not monitored on a large scale throughout the U.S., so annual recruitment estimates that represent the population we defined for our analysis are not available. Although there is historic information that *p.br* is close to 1 at low densities (Turrin 2014), we did not have any recent study-specific data available to inform how *p.br* may be changing with recent population increases. Otto (In U.S. Fish and Wildlife Service 2016a) conducted a meta-analysis of bald eagle productivity (i.e., young fledged per occupied nest) data using 17 regional studies conducted from 1995 to 2014 within our study area. He estimated median productivity was 1.12 (95%CI = 0.73-1.72), which we used to inform *F* in our IPM.

Two large-scale surveys, the North American Breeding Bird Survey (BBS; Robbins et al. 1986) and eBird (Fink et al. 2020), provide indices to bald eagle population sizes in areas where nest occupancy surveys occurred, and areas outside of that survey's coverage. The BBS is conducted each spring by volunteers that record birds along assigned roadside routes throughout our study area and other portions of North America. Each route is 39.4 km long and observers stop every 0.8 km for 3 minutes to record birds heard or seen within 400 m. The BBS is conducted between April and June and counts are conducted between 30 minutes before sunrise and 4 hours after. Full details of survey design and field methods for the BBS are provided by Robbins et al. (1986). Juvenile bald eagles are likely still in the nest when the BBS is conducted over most of the country and, therefore, are not likely to be counted during the survey. eBird is a citizen-science database consisting of checklists recorded by birders throughout the U.S. and throughout the year (Sullivan et al. 2009). Counts of birds, location, time, and search effort are standardized so that relative comparisons can be made among locations and time periods. Checklists are filtered and managed by birding experts to identify errors and maintain the quality of the information submitted (Sullivan et al. 2014). Because of the extensive controls and checks, the use of eBird data to inform scientific investigations and bird management is increasing (e.g., Sullivan et al. 2017, Robinson et al. 2018, Callaghan et al. 2019). In contrast to the nest-occupancy survey, the BBS and eBird indices do not provide population size estimates, but they cover a larger area and include subadults and adult floaters providing a more complete picture of spatial and temporal variation in bald eagle relative abundances.

The IPM we developed for bald eagles is based on three submodels: (1) a survival submodel using band recovery data; (2) a recruitment submodel based on a meta-analysis from published studies of productivity (Otto, In U.S. Fish and Wildlife Service 2016a) and an assumed relationship between density and the probability of breeding; and (3) a stage-structured model (Caswell 2001) that combines age-specific survival and recruitment estimates with time series data from the BBS conducted each spring. We used a state-space (Buckland et al. 2004, Kéry and Schaub 2012) formulation to integrate the BBS and demographic data because it allowed us to model the true latent state, and the observation process using the annual BBS indices and standard errors. Our IPM included four age classes: first-year (Y1), second-year (Y2), third-year (Y3), and after third-year (AY3). We assumed that eagles surviving their first year had the same survival rate after the first year (AY1) and that birds did not breed until their 4th spring after fledging (e.g., Y3 birds that transition to AY3 do not breed that first spring of turning an AY3 bird; U.S. Fish and Wildlife Service 2016a). We used a post-breeding matrix model (Caswell 2001) to represent the age-structured population dynamics:

$$\begin{bmatrix} 0 & 0 & 0 & S_.^{AY1} \times p.\,br_t \times F_t \\ S_t^{Y1} & 0 & 0 & 0 \\ 0 & S_.^{AY1} & 0 & 0 \\ 0 & 0 & S_.^{AY1} & S_.^{AY1} \end{bmatrix} \times \begin{bmatrix} I_t^{Y1} \\ I_t^{Y2} \\ I_t^{Y3} \\ I_t^{AY3} \end{bmatrix} = \begin{bmatrix} I_{t+1}^{Y1} \\ I_{t+1}^{Y2} \\ I_{t+1}^{Y3} \\ I_{t+1}^{AY3} \end{bmatrix}$$

Where S_t^{Y1} and S^{AY1} represent age-specific survival (see details of survival submodel below), $p.\,br_t$ is the probability of AY3 birds breeding, F_t is fecundity (juvenile females fledged per breeding female), and I_t^{Age} are the annual age-specific latent indices to population size. A subscript "t" means we allowed the parameter to vary annually, whereas a subscript "." indicates that the mean value was used in the state-space process model of IPM. We used the R package 'popbio' (Stubben and Milligan 2007) to estimate the sensitivities and elasticities of the medians from the posterior distributions of the lower-level demographic parameters used in the IPM to measure the relative influence of the demographic parameters on growth rate. We also explored transient dynamics by calculating the damping ratio, and simulating growth with an initial equal number of individuals in each age class to estimate years to a stable age distribution.

Survival

We used the Seber parameterization of dead recovery models (see Williams et al. 2002:398) to estimate survival rates. This parameterization includes band recoveries throughout the year and estimates age-specific survival (S) and a reporting probability (r), which is defined as the probability that a dead bird is encountered, and its band is reported to the Bird Banding Lab.

Banding of AY1 birds occurred continuously throughout the year, so we considered each time interval to start immediately after banding for this age class (i.e., the month and day of banding defines each subsequent survival interval for that individual). For example, if one eagle was banded on 1 June 2010, the first annual interval for that bird would be 1 June 2010 to 31 May 2011; whereas the interval for a bird banded on 1 Oct 2010 would be 1 Oct 2010 to 30 Sept 2011. Therefore, our time steps for AY1 were intervals since banding, which did not overlap completely among individuals or align with calendar years. We were concerned that our approach for setting intervals for AY1 could bias Y1 survival probabilities. For example, the interval survival for a Y1 eagle banded in May would be lower than a Y1 eagle banded in November because the bird banded in November would spend a longer portion of the interval as an AY1 if the birds transitioned to the next age class during the spring following banding. Approximately 80% of Y1 birds were banded in May and June, so we filtered the Y1 bandings to include just those banded during these two months to keep the time period consistent for all Y1 birds. Checking nest success of raptors often occurs just before chicks fledge (Steenhof and Newton 2007), which is when most banders target Y1 eagles for marking. Therefore, we assumed that survival between banding and fledging was ~1 for Y1 eagles. We also assumed that any Y1 birds observed after the 1st of March of the year following birth, had transitioned to the AY1 age class. Therefore, the Y1 survival rate represented an approximate 275-day period (i.e., approximately 0.75 of a year) rather than the year-long survival rate of AY1. This enabled us to avoid overlap between AY1 and Y1 survival rate estimates.

We used a logit link and allowed a random year-effect for survival for Y1 birds:

$$logit(S_t^{Y1}) = \beta_o + Y$$

The intercept (β_o) represents the mean $S_.^{Y1}$ and Y represents the random year affects, which we sampled from a normal distribution:

$$Y \sim N(0, \sigma^2_{year})$$

We used estimates of S_t^{Y1} from the random effects model in the IPM. Because of the continuous banding of AY1, we did not have clear annual cycles, and assumed constant survival and estimated a mean $S_.^{AY1}$ to use in the IPM. We do not think this is an unreasonable assumption for our analysis since this parameter is high and likely not very variable among years (Newton et al. 2016). We specified non-informative priors for each parameter used to inform survival: $\beta_o \sim N(0,1000000)$, $S_.^{AY1} \sim BETA(1,1)$, and $\frac{1}{\sigma^2_{year}} \sim GAMMA(0.001,0.001)$. We also used non-informative priors for Y1 and AY1 reporting rates: $r_.^{age} \sim BETA(1,1)$. We summarized the data in recovery arrays and used a multinomial likelihood to analyze the dead recovery data. As part of model checking, we compared survival rates from the full IPM to those from a stand-alone survival model (i.e., the same Seber dead recovery model) to assess whether other data sources in the IPM may have influences survival rates.

Recruitment

The first component of our recruitment estimate is the probability of AY3 birds breeding ($pr.br_t$). Previous research indicates that density dependence on recruitment would influence raptors through this parameter (Hunt 1998, Turrin 2014, Millsap et al. 2019). Therefore, we specified a logit-linear relationship between $pr.br_t$ and latent population indices (I_t^{All}):

$$logit(pr.br_t) = \beta_O + \beta_1 \times I_t^{All}$$

We did not have data to directly estimate the parameters in this model, so we included more informative priors than for the other parameters in the model, and then allowed the structure of the IPM to generate posterior estimates. We assumed that at low densities, most AY3 birds will attempt to breed each year (Turrin 2014), so we set $\beta_O = 5$. We did not have prior information on the slope parameter, but assumed that the probability of breeding would only go down with increasing population size and specified an informed prior for the slope parameter that covered the range of biologically relevant patterns: $\beta_1 \sim UNIFORM(-1,0)$. We did not have annual estimates of fecundity (F_t) to include in our IPM, so we sampled values from a distribution defined by the parameters from the meta-analysis (Otto In U.S. Fish and Wildlife Service 2016a) for annual estimates. First, we used the package "fitdistrplus" (Delignette-Muller and Dutang 2015) in program R to convert the median and credible interval for productivity in the meta-analysis (Otto, In U.S. Fish and Wildlife Service 2016a) to estimate a standard error on the lognormal scale ($\bar{x} = 0.12$; sd = 0.21) since productivity cannot be <0 and the standard error from the meta-analysis was skewed to the right. We sampled from this distribution within the MCMC updates in the IPM. For each value sampled, we divided by 2 to convert the productivity (fledglings per occupied nest), to a F_t (females fledged per breeding female) assuming a 50:50 sex ratio of fledglings (Bortolotti 1986).

BBS and stage-structured model

We used annual population indices for the combination of state and BCR from the BBS survey derived from a log-linear hierarchical model (Sauer et al. 2017). The log-linear model

incorporates observer, route, experience (i.e., first time observer vs not first time), year, and strata (state-BCR intersections) effects. The final indices from the BBS are the average number of birds seen per route for each stratum and year. Although we would prefer to have a time series of population size estimates rather than indices, the other parameters (e.g., survival and recruitment) in our IPM are rates, so as long as the BBS indices accurately capture population dynamics from one year to the next, they provide an appropriate time series to include in our IPM (e.g., Ahrestani et al. 2017, Robinson et al. 2018). Each year, the BBS indices are produced with an estimate and standard error that can be aggregated to various larger scales.

The underlying state model is based on the expansion of the matrix model above and the vector of un-measurable latent age-specific indices:

$$I_{t+1}^{Y1} = I_t^{AY3} \times S_.^{AY1} \times p.br_t \times F_t$$

$$I_{t+1}^{Y2} = I_t^{Y1} \times S_.^{Y1}$$

$$I_{t+1}^{Y3} = I_t^{Y2} \times S_.^{AY1}$$

$$I_{t+1}^{AY3} = (I_t^{Y3} \times S_.^{AY1}) + (I_t^{AY3} \times S_.^{AY1})$$

We made two adjustments to the BBS indices to integrate them into observation process. Observers cannot identify age class (i.e., Y2 vs Y3 vs AY3) during surveys, so the observed indices ($I.obs_t$) are not age-specific, whereas survival and fecundity varied among some of the age-specific latent indices in the state model (i.e. I_t^{Y1}, I_t^{Y2}, I_t^{Y3}, and I_t^{AY3}). We allocated the latent total I_1 into age-specific estimates (i.e., vector $\boldsymbol{I_t^{age}}$) using the stable-age distribution, calculated from mean survival and recruitment from a literature search of previous studies (Buehler et al. 1991, Harmata et al. 1999, Buehler 2020). We used a Dirichlet distribution with the stable age distribution as priors for the first year to ensure the proportion of age classes (i.e., p_t^{Y1}, p_t^{Y2}, p_t^{Y3}, and p_t^{AY3}) summed to 1. We then used the age-specific demographic rates to calculate age-specific indices at the end of time $t = 1$ and calculated updated proportions in each age class each year. During each time step t in the model, the current estimate of age-specific indices was the previous year's total (I_{t-1}) multiplied by the proportion of birds in each class from the end of the previous year. The Y1 survival and recruitment estimates were based on a post-breeding time schedule, whereas, the BBS surveys are conducted during the nesting periods when juveniles are not generally available to be counted. To match the survey and demographic data, we summed the latent indices for Y2, Y3, and AY3:

$$I.BBS_t = I_t^{Y2} + I_t^{Y3} + I_t^{AY3}$$

in the state model so that we could match with the observed BBS indices in the observation model:

$$I.obs_t \sim N(I.BBS_t, \sigma_{I.BBS_t}^2)$$

Estimating $\widetilde{N}_{2018}$

The occupied nest survey data were integrated with eBird data (see Part 2) to get an estimate of the total number of occupied nests for 2018 (N_{2018}^{Nests}). Researchers developed a model that estimates a scaling factor using eBird data and plot-level estimates from the nest occupancy survey where the two surveys overlap spatially Part 2). Their model also incorporated a random

effect for strata to accommodate variation in the scaling factor associated with habitat. The model was then used to scale eBird data to an estimate of breeding occupancy over the entire study area. The eBird data prior to 2018 could not be scaled to a breeding population size because only the 2018 eBird data were processed as needed for scaling to a nest occupancy estimate. Although eBird data includes both nesting and non-nesting birds, the inferences from the integrated eBird and nest occupancy estimates represent number of nests only because the eBird data are scaled to nest occupancy data in overlap areas (i.e., the scaling factors scale eBird indices to the number of occupied nests). Because our take assessment required nesting and non-nesting eagles, we doubled the integrated eBird/post-delisting estimate of occupied nests (i.e., assumed two adults per nest), and adjusted by the proportion of breeders and non-AY3 birds from our IPM.

$$\widetilde{N}_{2018} = \frac{N_{2018}^{Nests} \times 2}{p.br_{2018} \times p_{2018}^{AY3}}$$

We used simulations to sample values of $p.br_{2018}$ and p_{2018}^{AY3} from the posterior estimates of the IPM, and the variance in N_{2018}^{Nests} (Part 2) to propagate uncertainty to our overall estimate of $\widetilde{N}_{2018}$. Our estimate of $p.br_{2018}$ was not informed directly by data and was, therefore, highly uncertain. Therefore, we sampled values for this parameter from within the 90% CI to ensure that unreasonable breeding proportions did not lead to implausible population size estimates. Therefore, the final N included breeding and non-breeding eagles from all regions within the conterminous U.S.

RESULTS

Survival Submodel

After filtering bands, we had a total of 12,573 Y1 (range = 238 – 776 annually) and 3,259 AY1 (range = 78 – 198, annually) eagles banded between 1994 and 2018 for our dead recovery analysis. We had very few dead recoveries during the study, particularly for AY1 (total Y1 recoveries = 1275, range = 9 – 81 annually; and total AY1 recoveries = 345, range = 1 – 37 annually). Reporting rate estimates were low and precise for both age classes ($\hat{r}^{Y1}$= 0.06, 95% CI (Bayesian) = 0.04 – 0.08; $\hat{r}^{AY1}$= 0.19, 95% CI = 0.17 – 0.21). Survival probabilities for Y1 varied temporally from 0.68 (95% CI = 0.56 – 0.78) to 0.74 (95% CI = 0.65 – 0.86) and appeared stable over much of the study period (Figure 2). Although the survival estimates of Y1 varied from year to year, the low precision of annual estimates from the random-effects model indicated that these temporal differences were not strong as illustrated by overlapping credible intervals for all annual estimates (Figure 3). The mean survival estimate for AY1 was high and precise ($\hat{S}^{AY1}$= 0.91, 95% CI = 0.0.90 – 0.92). We found that annual survival rates for Y1 from the IPM and the stand-alone Seber model with the same structure showed the same temporal patterns, but were lower ($\hat{\bar{S}}_{IPM}^{Y1}$= 0.70 [95% CI = 0.63 – 0.79], $\hat{\bar{S}}_{StandAlone}^{Y1}$= 0.77 [95% CI = 0.68 – 0.87]). The mean AY1 survival from the stand-alone Seber model ($\hat{\bar{S}}_{StandAlone}^{AY1}$= 0.92, 95% CI = 0.91 – 0.93) was also slightly higher than the estimate from the IPM.

Recruitment Submodel

The median of the slope parameter relating the proportion of AY3 birds that breed to the population index was -21 (95% CI = -0.34 – -0.01) with high uncertainty (CV = 47%). The IPM indicated that the estimated proportion of AY3 birds breeding declined from approximately 0.990 (95% CI = 0.986 – 0.993) to 0.66 (95% CI = 0.16 – 0.99) by the end of the study (Figure 3). Annual fecundity estimates from the IPM only varied slightly with no apparent trend (range $\hat{F}$ = 0.52 to 0.59; Figure 5) and were almost identical to the expected values from the priors (E(F) = 0.57, SD = 0.12). Based on the assumption that density dependence acts through the proportion of AY3 eagles breeding, our full IPM indicated that overall recruitment in our study declined from 0.53 (95% CI = 0.36 – 0.78) to 0.37 (95% CI = 0.09 – 0.72) as the overall population increased from 1994 to 2018 (Figure 4).

State Model

The distribution of age classes did not fluctuate among years, with AY3 consistently being highest ($\hat{\bar{p}}^{AY3}$ = 0.53; range $\hat{p}^{AY3}$ = 0.50 to 0.57), followed by Y1 ($\hat{\bar{p}}^{Y1}$ = 0.22; range $\hat{p}^{Y1}$ = 0.16 to 0.23), and then subadults: ($\hat{\bar{p}}^{Y2}$ = 0.14 range $\hat{p}^{Y2}$ = 0.10 to 0.15) and ($\hat{\bar{p}}^{Y3}$ = 0.12; range $\hat{p}^{Y3}$ = 0.08 to 0.12). These proportions were in the same order as predicted from the stable-age distribution based on a literature search with adults expected to make up the highest proportion ($\hat{p}^{AY3}$ = 0.57), followed by Y1 ($\hat{p}^{Y1}$ = 0.18), and then subadults ($\hat{p}^{Y2}$ = 0.14, and $\hat{p}^{Y3}$ = 0.11). Although the order was the same, the fitted age proportions derived from the IPM from year 2 to the end of the analysis indicated a slightly higher proportion of Y1 and lower proportion of AY3 than the stable-age distribution used as a prior in year 1 of the analysis.

The latent estimates of population indices for subadult (Y2 and Y3) and AY3 bald eagles indicated that the population in our study increased rapidly since 1994 at a rate of approximately 10% per year (Figure 5). The latent population indices were similar to the observed BBS data, and the annual estimates were precise ($\overline{CV}$ = 6%, range = 5% to 7%; Figure 6). Because the proportion of Y1 in the population did not fluctuate much throughout the study, the full population index that included that age class had a similar trend with an offset of about +25% (Figure 5).

Growth rate from the population model using the median of the posterior distributions of demographic rates was most sensitive to $\hat{S}^{AY1}$ (sensitivity = 1.08, elasticity = 0.88), followed by F (sensitivity = 0.24, elasticity = 0.16), $\hat{S}^{Y1}$ (sensitivity = 0.18, elasticity = 0.12), and $p.br$ (sensitivity = 0.14, elasticity = 0.12). The estimated damping ratio was 1.70 and simulation of the matrix indicated that a population with equal numbers of birds in each age class would converge to the stable age distribution within 5 years.

Adjusting the integrated eBird and nest occupancy surveys described in Part 2 for the number of nesting birds (i.e., 2 × nesting pairs), proportion of birds breeding (to add AY3 floaters) and proportion of Y1, Y2, and Y3 birds (Table 1) increased estimates by approximately 4.4 times from previous population size estimate.

DISCUSSION

Our IPM provided several insights into bald eagle demography that would not have been evident otherwise. Most significantly, the IPM allowed us to estimate the proportion of AY3 bald eagles that were breeding each year in the absence of direct information on that demographic component. Moffat's equilibrium theory (Hunt 1998, 2015, Hunt and Law 2000) predicts that the availability of suitable breeding locations places an upper limit on the number of mature individuals that can reproduce annually, and thus is a primary means of population regulation in long-lived species of Accipitriformes like bald eagles. Turrin (2014) showed that mature bald eagles that were unable to secure breeding territories (i.e., floaters) comprised an insignificant proportion of the bald eagle population in the Chesapeake Bay region in the early 1990's when breeding density was low due to population declines associated with DDT contamination (Buehler 2020). By 2013, however, after 40 years of bald eagle population growth following cessation of the use of DDT in the U.S., only one in five four-year old bald eagles in the Chesapeake Bay region was able to secure a breeding territory (Turrin 2014). Our IPM revealed that this same pattern is occurring more broadly across the U.S., with the proportion of AY3 bald eagles that are breeding decreasing concomitantly with continued population growth at that larger scale; currently, we estimate that only about 70% of adult bald eagles are associated with nesting territories in the conterminous U.S. By being able to account for the sizable pool of adult bald eagles not associated with nesting territories, we were able to estimate a more accurate population size.

The IPM accounted for floaters indirectly, with no observation data to inform the estimates of *p.br*. This resulted in substantial uncertainty, but the trends and magnitude of the estimates were plausible and consistent with the information available from local studies (Hansen and Hodges 1985, Turrin 2014, Turrin and Watts 2015). To obtain reasonable estimates, we constrained *p.br* by setting the intercept of 5 on the logit scale (i.e. *p.br* approximately 1) and using a partially-informed prior on the slope parameter. By using a uniform prior on the slope parameter for *p.br*, that kept estimates between 0.88 and 1.0 at low densities, we were able to contain the uncertainty in our estimates of *p.br*, as well as in other parameters that it contributed to (e.g., *N*). Given that our estimates of *p.br* for the most recent years in our time series are lower than the range estimated at extremely low densities implies that information from other vital rates is providing useful information on breeding propensity and driving this parameter downward. Although we explored a range of biologically reasonable priors, in the future it might be worth exploring other specifications for priors for the parameters in the propensity for the breeding submodel to see if lower levels of breeding propensity with reasonable bounds on uncertainty are indicated.

Our IPM also allowed us to generate slightly more precise estimates of bald eagle survival, particularly for Y1, than with independent survival models. Survival rates of bald eagles have not been widely studied, and our results and those of the U.S. Fish and Wildlife Service (2016a) are the only range-wide estimates available. Our IPM-based estimate of AY1 survival (0.91) is within the range of estimates from previous local studies (0.50 – 0.95; McCollough 1986, Buehler et al. 1991, Gerrard et al. 1992, Wood 1992, Bowman et al. 1995, Hodges et al. 1987, Harmata et al. 1999, Millsap et al. 2004). Our estimate of mean Y1 survival (0.70), however, is at the lower end of the range from previous studies (0.67 – 0.92; Buehler et

al. 1991, Gerrard et al. 1992, Wood 1992, Bowman et al. 1995, Harmata et al. 1999, Millsap et al. 2004). One factor that might explain the lower Y1 survival rate that we found is that our analysis incorporated data from some substantial parts of the bald eagle's range not included among the previous regional analyses. In particular, our analysis included the results from extensive banding of nestlings in the Great Lakes and upper Midwest regions, where many bald eagles are migratory. Buehler (2020), in his review of bald eagle survival information through 1999, noted there was some evidence that survival of juvenile bald eagles from migratory populations might be lower than those from sedentary populations.

Our sensitivity analysis indicated that survival, particularly adult survival, likely has the greatest influence of any vital rate on bald eagle population growth (Grier 1980), hence, an accurate estimate of this parameter is especially important in estimating population trajectory. Fortunately, adequate numbers of bald eagles have been banded in the U.S. to allow direct estimates of survival rates, including the ability to infer annual estimates of Y1 survival using a random effects model (Fay et al. 2020). In addition, in future updates to the IPM, annual estimates of the number of breeding pairs of bald eagles should be available from the integrated eBird and occupied nest model, allowing for the direct estimation of annual population size as opposed to an index of population size, which we used here. The finer scale of eBird estimates should also further contribute to increased precision in other parameter estimates from the IPM. However, other vital rates can also have important effects on population dynamics. For example, as noted above, in large raptors, fecundity is the parameter most likely affected by density dependence. Information on bald eagle fecundity was not available at sufficient spatial and temporal scales to allow us to directly incorporate such variation in our IPM. Sensitivity analyses and other assessments of the comparative value of the data used in our IPM and PTL models would be helpful in prioritizing the allocation of effort for future studies of bald eagle population dynamics. We suspect that by being able to account even coarsely for annual variation in mean brood size, our IPM would be better able to estimate the proportion of adults that breed and thus account for density dependence. Collecting such information would be time intensive and costly; however, an assessment of the value the data would provide for informing management decisions should be conducted before investing effort into gathering it.

ACKNOWLEDGEMENTS

LITERATURE CITED

Abadi, F., O. Gimenez, R. Arlettaz, and M. Schaub. 2010. An assessment of integrated population models: Bias, accuracy, and violation of assumptions. Ecology 91:7-14.

Abadi, F., O. Gimenez, H. Jakober, W. Stauber, R. Arlettaz, and M. Schaub. 2012. Estimating the strength of density dependence in the presence of observation errors using integrated population models. Ecological Modelling 242:1-9.

Ahrestani, F. S., J. F. Saracco, J. R. Sauer, K. L. Pardieck, and J. A. Royle. 2017. An integrated population model for bird monitoring in North America. Ecological Applications 27: 916-924.

Besbeas, P., S. N. Freeman, B. J. T. Morgan, and E. A. Catchpole. 2002. Integrating mark-recapture-recovery and census data to estimate animal abundance and demographic parameters. Biometrics 58:540-547.

Bortolotti, G. R. 1986. Influence of Sibling Competition on Nestling Sex Ratios of Sexually Dimorphic Birds. The American Naturalist 127:495–507.

Bowman, T. D., P. F. Schempf, and J. A. Bernatowicz. 1995. Bald eagle survival and population dynamics in Alaska after the" Exxon Valdez" oil spill. The Journal of wildlife management 317–324.

Buckland, S. T., K. B. Newman, L. Thomas, and N. B. Koesters. 2004. State-space models for the dynamics of wild animal populations. Ecological Modelling 171:157-175.

Buehler, D. A., J. D. Fraser, J. K. D. Seegar, and G. D. Therres. 1991. Survival Rates and Population Dynamics of Bald Eagles on Chesapeake Bay. The Journal of Wildlife Management 55:608.

Buehler, D. A. 2020. Bald Eagle (*Haliaeetus leucocephalus*), version 1.0. In Birds of the World (A. F. Poole and F. B. Gill, Editors). Cornell Lab of Ornithology, Ithaca, NY, USA. https://doi.org/10.2173/bow.baleag.01

Callaghan, C. T., A. G. B. Poore, R. E. Major, J. J. L. Rowley and W. K. Cornwell. 2019. Optimizing future biodiversity sampling by citizen scientists. Proc Biol Sci 286(1912): 20191487.

Caswell, H. 2001. Matrix Population Models. Construction, Analysis, and Interpretation. Sinauer Associates, Inc. Sunderland, MA, USA.

Delignette-Muller ML, Dutang C (2015). "fitdistrplus: An R Package for Fitting Distributions." Journal of Statistical Software, 64(4), 1–34. http://www.jstatsoft.org/v64/i04/.

Fay, R., S. Michler, J. Laesser, J. Jeanmonod, and M. Schaub. 2020. Can temporal covariation and autocorrelation in demographic rates affect population dynamics in a raptor species? Ecology and Evolution 10:1959-1970.

Fink, D., T. Auer, A. Johnston, M. Strimas-Mackey, O. Robinson, S. Ligocki, B. Petersen, C. Wood, I. Davies, B. Sullivan, M. Iliff, S. Kelling. 2020. eBird Status and Trends, Data Version: 2018; Released: 2020. Cornell Lab of Ornithology, Ithaca, New York. https://doi.org/10.2173/ebirdst.2018

Gerrard, J. M., P. N. Gerrard, P. N. Gerrard, G. R. Bortolotti, and E. Z. Dzus. 1992. A 24-year study of bald eagles on Besnard Lake, Saskatchewan. Journal of Raptor Research 26:159-166.

Grier, J. W. 1980. Modeling approaches to bald eagle population dynamics. Wildlife Society Bulletin 316–322.

Hansen, A. J. and J. I. Hodges, Jr. 1985. High rates of nonbreeding adult bald eagles in southeast Alaska. Journal of Wildlife Management 49:454-458.

Harmata, A. R., G. J. Montopoli, B. Oakleaf, P. J. Harmata, and M. Restani. 1999. Movements and survival of bald eagles banded in the Greater Yellowstone Ecosystem. The Journal of Wildlife Management 781–793.

Hodges, J. I., E. L. Boeker, and A. J. Hansen. 1987. Movements of radio-tagged bald eagles, *Haliaeetus leucocephalus*, in and from southeast-ern Alaska. Canadian Field-Naturalist 101:136- 140.

Hunt, W. G. 1998. Raptor floaters at Moffat's equilibrium. Oikos 82:191–197.

Hunt, W. G. and P. R. Law. 2000. Site-dependent regulation of population size: Comment. Ecology 81:1162-1165

Hunt, W. G. 2015. C. B Moffat's anticipation of twenty-first century bird population dynamics theory. Ibis 157:888-891.

Hunt, W. G., J. D. Wiens, P. R. Law, M. R. Fuller, T. L. Hunt, D. E. Driscoll, and R. E. Jackman. 2017. Quantifying the demographic cost of human-related mortality to a raptor population. PLoS ONE 12(2): e0172232. doi:10.1371/journal.pone.0172232.

Kéry, M., and M. Schaub. 2012. Bayesian Population Analysis using WinBUGS. A Hierarchical Perspective. Academic Press, NY, USA.

Koneff, M.D., G.S. Zimmerman, C.P. Dwyer, K.K. Fleming, P.I. Padding, P.K. Devers, F.A. Johnson, M.C. Runge, and A.J. Roberts. 2017. Evaluation of harvest and information needs for North American sea ducks. PloS One 12.

McCollough, M. R. 1986. Post-fledging ecology and population dynamics of bald eagles in Maine. Dissertation, University of Maine, Orono, Maine, USA.

Millsap, B. A., Breen, T., E. McConnell, T. Steffer, L. Phillips, N. J. Douglass, and S. Taylor. 2004. Comparative fecundity and survival of bald eagles fledged from suburban and rural natal areas in Florida. The Journal of Wildlife Management 64:1018–1031.

Millsap, B. A., and G. T. Allen. 2006. Effects of falconry harvest on wild raptor popualtions in the United States: Theoretical considerations and management recommendations. Wildlife Society Bulletin 34:1392-1400.

Millsap, B. A., K. Madden, R. K. Murphy, M. Brennan, J. E. Pagel, D. Campbell, and G. W. Roemer. 2019. Demographic consequences of sexual differences in age at first breeding in Cooper's Hawks (*Accipiter cooperii*). The Auk 136: 1–20. https://doi.org/10.1093/auk/ukz032

Millsap, B. A., G. S. Zimmerman, W. L. Kendall, J. G. Barnes, M. A. Braham, B. E. Bedrosian, D. Bell, P. H. Bloom, R. H. Crandall, R. Domenech, D. Driscoll, A. E. Duerr, R. Gerhardt, S. E. J. Gibbs, A. R. Harmata, K. Jacobson, T. E. Katzner, R. N. Knight, C.

McIntyre, R. K. Murphy, S. J. Slater, B. W. Smith, J. P. Smith, D. W. Stahlecker, J. W. Watson. In Prep. Age-specific survival rates, causes of death, and allowable take of golden eagles in the western United States.

Newton, I., M. J. McGrady, and M. K. Oli. 2016. A review of survival estimates for raptors and owls. Ibis 158:227–248.

Robbins, C. S., D. Bystrak, and P. H. Geissler. 1986. The Breeding Bird Survey: its first fifteen years, 1965–1979. U.S. Fish and Wildlife Service Resource Publication 157, Washington, D.C., USA.

Robinson, O. J., V. Ruiz-Gutierrez, D. Fink, R. J. Meese, M. Holyoak, and E. G. Cooch. 2018. Using citizen science data in integrated population models to inform conservation. Biological Conservation 227:361-368.

Sauer, J. R., D. K. Niven, J. E. Hines, D. J. Ziolkowski, Jr, K. L. Pardieck, J. E. Fallon, and W. A. Link. 2017. The North American Breeding Bird Survey, Results and Analysis 1966 - 2015. Version 2.07.2017 USGS Patuxent Wildlife Research Center, Laurel, MD.

Steenhof, K. and I. Newton. 2007. Assessing Nesting Success and Productivity. Pages 181-192 *In* D. M. Bird and K. L. Bildstein, eds. Raptor Research and Management Techniques. Hancock House Publishers, Blaine, WA, USA.

Steenhof, K., M. N. Kochert, C. L. McIntyre, and J. L. Brown. 2017. Coming to terms about describing golden eagle reproduction. Journal of Raptor Research 51:378-390.

Stubben, C. J., and B. G. Milligan. 2007. Estimating and analyzing demographic models using the popbio package in R. Journal of Statistical Software 22:11.

Sullivan, B. L., C. L. Wood, M. J. Iliff, R. E. Bonney, D. Fink, and S. Kelling. 2009. eBird: a citizen-based bird observation network in the biological sciences. Biological Conservation 142: 2282-2292.

Sullivan, B. L., J. L. Aycrigg, J. H. Barry, R. E. Bonney, N. Bruns, C. B. Cooper, T. Damoulas, A. A. Dhondt, T. Dietterich, A. Farnsworth, D. Fink, J. W. Fitzpatrick, T. Fredericks, J. Gerbracht, C. Gomes, W. M. Hochachka, M. J. Iliff, C. Lagoze, F. A. La Sorte, M. Merrifield, W. Morris, T. B. Phillips, M. Reynolds, A. D. Rodewald, K. V. Rosenberg, N. M. Trautmann, A. Wiggins, D. W. Winkler, W.-K. Wong, C. L. Wood, J. Yu and S. Kelling. 2014. The eBird enterprise: An integrated approach to development and application of citizen science. Biological Conservation 169: 31-40.

Sullivan, B. L., T. Phillips, A. A. Dayer, C. L. Wood, A. Farnsworth, M. J. Iliff, I. J. Davies, A. Wiggins, D. Fink, W. M. Hochachka, A. D. Rodewald, K. V. Rosenberg, R. Bonney and S. Kelling. 2017. Using open access observational data for conservation action: A case study for birds. Biological Conservation 208: 5-14.

Turrin, C. 2014. Rise of a floater class. Master of Science Thesis. College of William and Mary, Williamsburg, Virginia, USA

Turrin, C., and B. D. Watts. 2015. Nest guarding in Chesapeake Bay bald eagles. Journal of Raptor Research 49:18-28.

U.S. Fish and Wildlife Service. 2007. Endangered and Threatened Wildlife and Plants; Removing the Bald Eagle in the Lower 48 States from the List of Endangered and Threatened Wildlife. Federal Register 72(130):37346-37372.

U.S. Fish and Wildlife Service. 2009. Post-delisting Monitoring Plan for the Bald Eagle (*Haliaeetus leucocephalus*) in the Contiguous 48 States. U.S. Fish and Wildlife Service, Divisions of Endangered Species and Migratory Birds and State Programs, Midwest Regional Office, Twin Cities, Minnesota.

U.S. Fish and Wildlife Service. 2016a. Bald and Golden Eagles: Population demographics and estimation of sustainable take in the United States, 2016 update. Division of Migratory Bird Management, Washington D.C. USA https://www.fws.gov/migratorybirds/pdf/management/EagleRuleRevisions-StatusReport.pdf

U.S. Fish and Wildlife Service. 2016b. Programmatic Environmental Impact Statement for the Eagle Rule Revision. U.S. Fish and Wildlife Service, Division of Migratory Bird Management, Washington, D.C. USA https://www.fws.gov/migratorybirds/pdf/management/FINAL-PEIS-Permits-to-Incidentally-Take-Eagles.pdf

U.S. Geological Survey Bird Banding Laboratory. 2019. North American bird banding and band encounter data set. Patuxent Wildlife Research Center, Laurel, MD. File Created 5/21/19.

Williams, B. K., J. D, Nichols, and M. J. Conroy. 2002. Analysis and Management of Animal Populations. Academic Press, SD, USA.

Wood, P. B. 1992. Habitat use, movements, migration patterns, and survival rates of subadult bald eagles in Florida. Dissertation, University of Florida, Gainesville, Florida, USA.

Table 1. Population size estimates of bald eagles by eagle management unit and total for the U.S. (excluding the southwestern U.S. and Alaska), 2018.

| Region | Population Size[1] | | |
	Mean	SD	Median (20th Quantile)
Atlantic Flyway	86,623	15,919	84,541 (72,990)
Central Flyway	31,183	5,754	30,427 (26,253)
Mississippi Flyway	163,680	30,093	159,772 (137,917)
Pacific Flyway - North	43,090	7,918	42,068 (36,302)
U.S. Total	324,515	59,665	316,708 (273,327)

[1]Calculated by multiplying occupied nests (from Part 2) by 2 and then dividing by proportion of breeders (to adjust for floaters) and the proportion of after third year birds to account for juveniles and subadults.
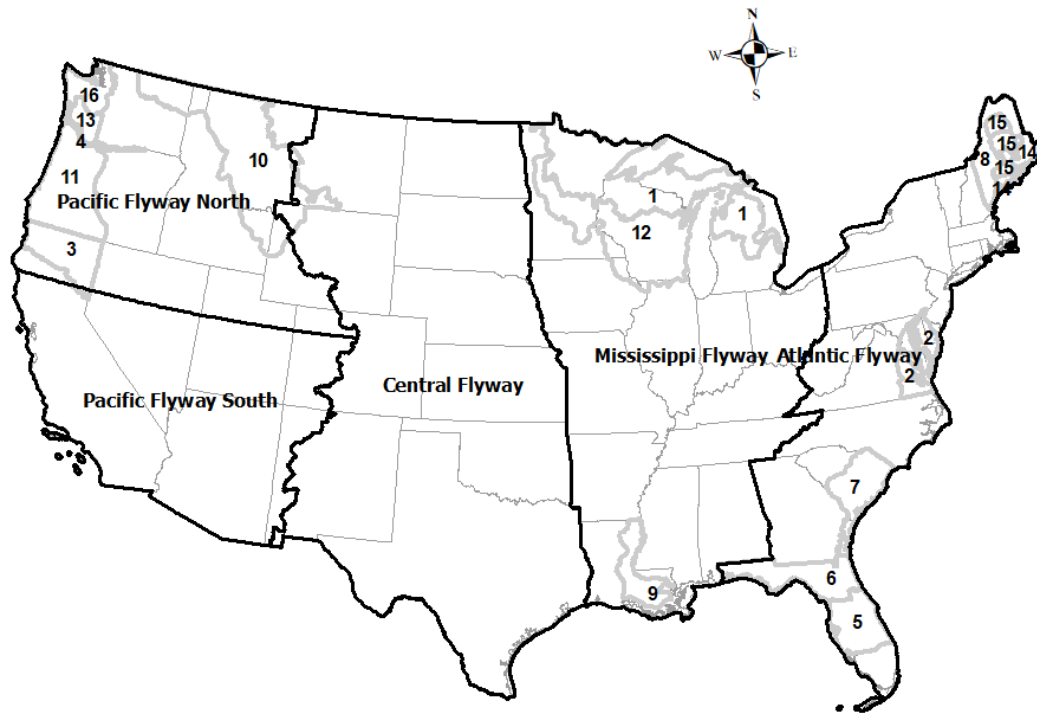
Figure 1. Bald eagle management units and survey strata. Management units are defined by the dark lines, and are labeled on the figure. Survey strata are 1 = Boreal Transition, 2 = Chesapeake Bay, 3 = California Highlands, 4 = Columbia River, 5 = Central Florida, 6 = Northern Florida, 7 = Southeastern Lowlands, 8 = Maine Lowlands, 9 = Mississippi Valley, 10 = Northern Rockies, 11 = Oregon, 12 = Prairie Transition, 13= Southern Cascades, 14 = Upper Atlantic Coast, 15= Maine Highlands, 16 = Western Cascades.
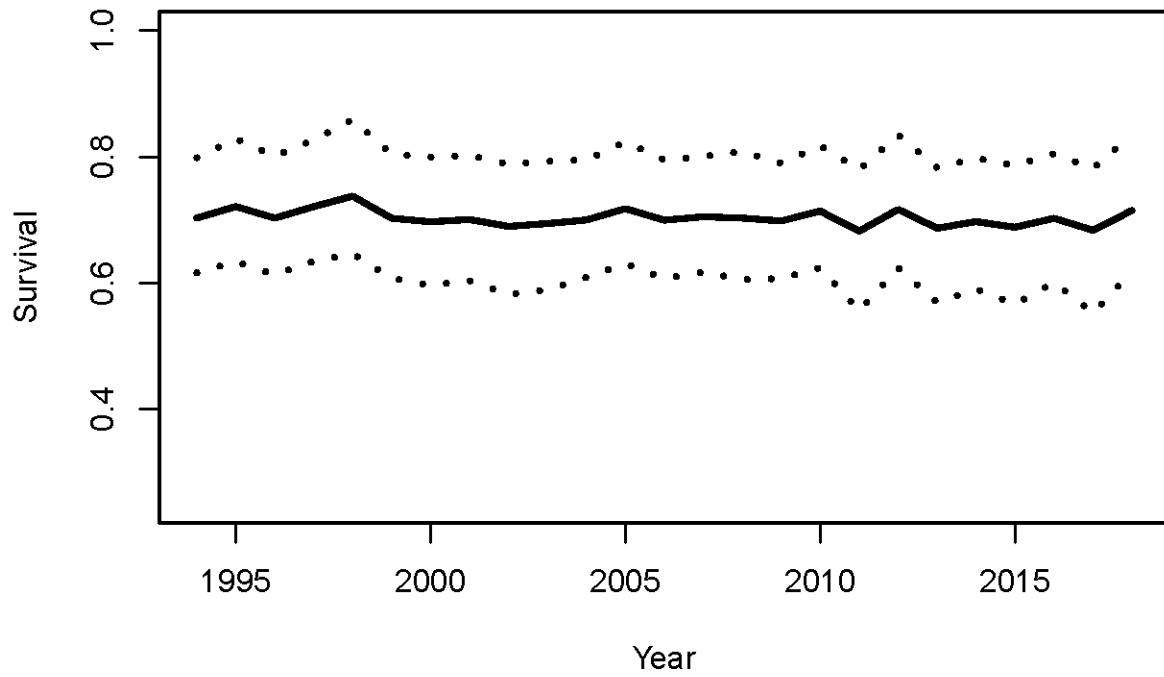
Figure 2. Juvenile (Y1) survival rates and 95% credible limits (dashed lines) of bald eagles in the conterminous U.S., excluding the southwestern U.S., based on band recoveries, 1994-2018.
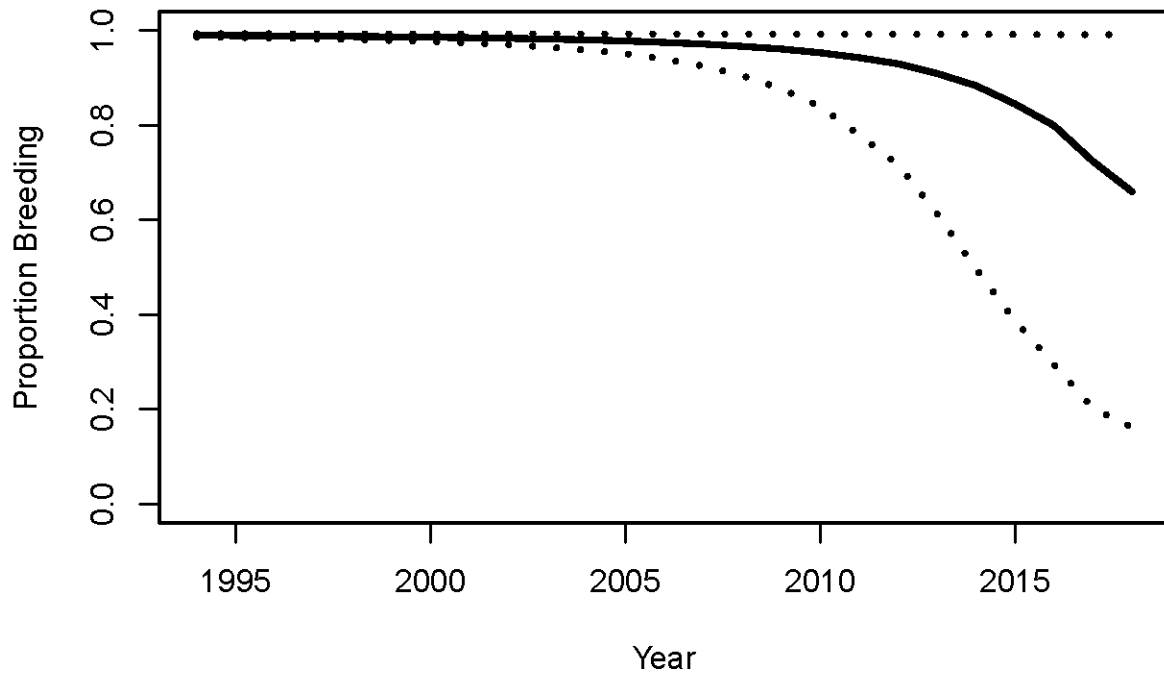
Figure 3. Estimated proportion, derived from an integrated population model, of after third-year bald eagles breeding and 95% credible limits (dashed lines) in the conterminous U.S., excluding the southwest, 1994-2018.
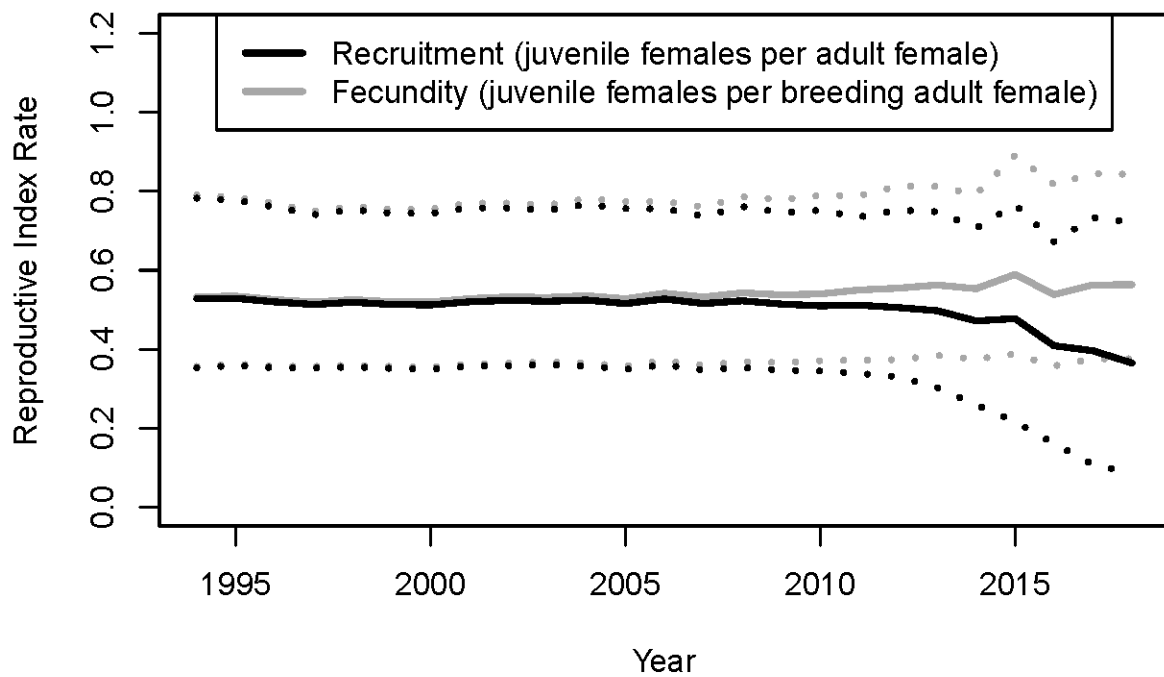
Figure 4. Estimated fecundity (Y1 females fledged per breeding AY3 female) and recruitment (Y1 females fledged per AY3 female) and 95% credible limits (dashed lines) for bald eagles in the conterminous U.S., excluding the southwest, 1994-2018.
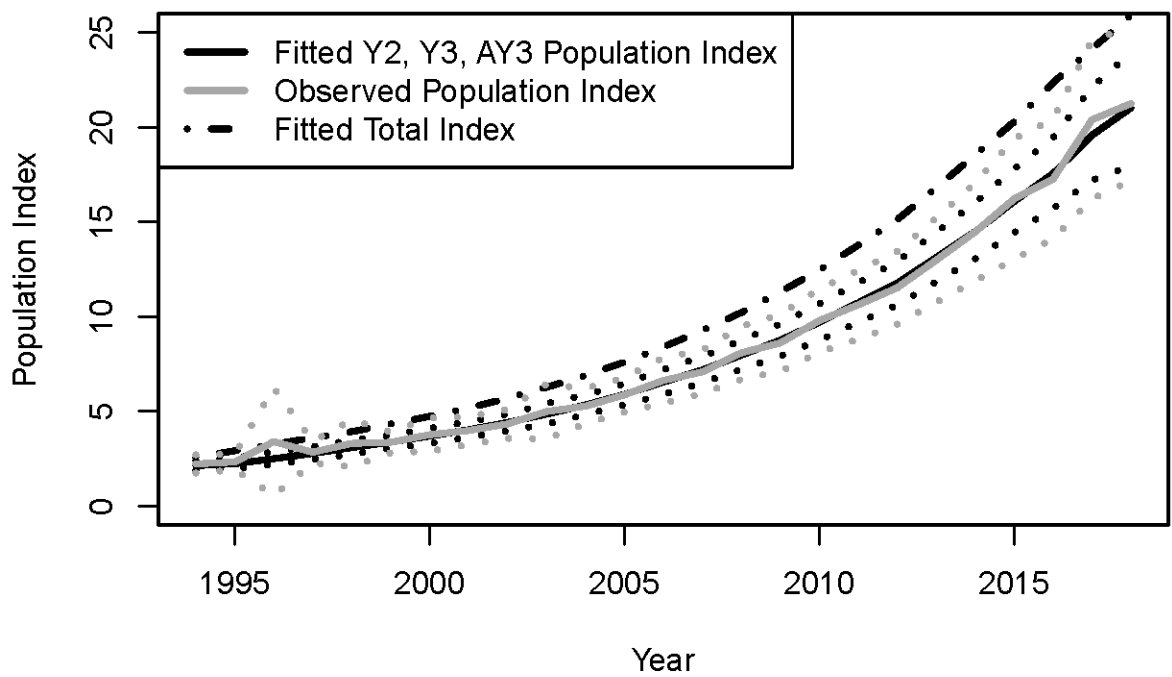
Figure 5. Observed Breeding Bird Survey (BBS) and fitted indices from an integrated population model of bald eagles in the conterminous U.S., excluding the southwest, 1994-2018. Y2, Y3, and AY3 are second-year, third-year, and after third-year age classes, respectively. BBS survey only detects these three age classes and total index includes juveniles. Short-dashed lines represent 95% credible limits.